



# Numerical investigation of TiO<sub>2</sub> and MWCNTs turbine meter oil nanofluids: Flow and hydrodynamic properties

Atiyeh Aghaei Sarvari, Saeed Zeinali Heris, Mousa Mohammadpourfard,  
Seyed Borhan Mousavi, Patrice Estellé

## ► To cite this version:

Atiyeh Aghaei Sarvari, Saeed Zeinali Heris, Mousa Mohammadpourfard, Seyed Borhan Mousavi, Patrice Estellé. Numerical investigation of TiO<sub>2</sub> and MWCNTs turbine meter oil nanofluids: Flow and hydrodynamic properties. *Fuel*, 2022, 320, pp.123943. 10.1016/j.fuel.2022.123943 . hal-03670044

**HAL Id: hal-03670044**

**<https://hal.science/hal-03670044>**

Submitted on 23 Sep 2022

**HAL** is a multi-disciplinary open access archive for the deposit and dissemination of scientific research documents, whether they are published or not. The documents may come from teaching and research institutions in France or abroad, or from public or private research centers.

L'archive ouverte pluridisciplinaire **HAL**, est destinée au dépôt et à la diffusion de documents scientifiques de niveau recherche, publiés ou non, émanant des établissements d'enseignement et de recherche français ou étrangers, des laboratoires publics ou privés.



Distributed under a Creative Commons Attribution - NonCommercial 4.0 International License

# Numerical investigation of TiO<sub>2</sub> and MWCNTs turbine meter oil nanofluids: Flow and hydrodynamic properties

Atiyeh Aghaei Sarvari<sup>a</sup>, Saeed Zeinali Heris<sup>a,\*</sup>, Mousa Mohammadpourfard<sup>a</sup>, Seyed

Borhan Mousavi<sup>b</sup>, Patrice Estellé<sup>c</sup>

<sup>a</sup> Faculty of Chemical and Petroleum Engineering, University of Tabriz, Tabriz, Iran

<sup>b</sup> Department of Mechanical Engineering, University of British Columbia, Vancouver,  
BC, Canada

<sup>c</sup> Univ Rennes, LGCGM, EA3913, F-35000 Rennes, France

\*Corresponding Author Email: [s.zeinali@tabrizu.ac.ir](mailto:s.zeinali@tabrizu.ac.ir)

## Abstract

The main aim of the present study is to evaluate the influence of multi-walled carbon nanotubes (MWCNTs) and TiO<sub>2</sub> nanoparticles (NPs) on lubricant and fluid flow within natural gas turbine meters. In light of this purpose, disparate concentration of TiO<sub>2</sub> NPs (0.1, 0.2, and 0.3 wt%), various volume flow rates 0.14, 0.35, and  $0.12 \frac{\text{cm}^3}{\text{s}}$  were employed for experimental analyses. In the facet of simulation, Gambit software version 2. 4. 6 to mesh oil pathway and Fluent software version for solving the equations were utilized. It was revealed that the pressure drop in the presence of nanoparticles was increased. Moreover, there was an increase in pressure drop value with raising the NPs concentration; for instance, the pressure drop value of MWCNTs-containing nanofluids at the volume flow rate of 0.35 cm enhanced from 92.72 Pa to 94.64 Pa as the NPs concentration raised from 0.1 to 0.3. Furthermore, modeling outcomes corroborated the uptrend in pressure drop value by increasing the volume flow rate and reported the maximum pressure drop value of  $0.12 \frac{\text{cm}^3}{\text{s}}$ . On the other hand, the numerical results revealed that the friction coefficient is directly and inversely proportional to NPs

concentration and the volume flow rates, sequentially. Additionally, with increasing the volume flow rate, the entrance length increased, and reaching the developed state was delayed. It is worth noting as the final finding of this study that increasing the NPs concentration resulted in decreasing the entrance length and the fast reaching of the developed state.

**Keywords:** Nanofluid; Lubricant; MWCNTs; TiO<sub>2</sub> nanoparticles; Gas turbine-meter; Pressure drop.

## Nomenclature

Q	Flow rate ( $\text{m}^3 \text{s}^{-1}$ )
U	Velocity ( $\text{m s}^{-1}$ )
A	Cross-section area ( $\text{m}^2$ )
K	Local energy dissipation coefficient
g	Gravitational acceleration ( $\text{m}^2 \text{s}^{-1}$ )
Re	Reynolds number
L	Length (m)
wt	Nanoparticle weight fraction (%)
D	Diameter (m)
P	Pressure ( $\text{kg m}^{-1} \text{s}^{-2}$ )
F	Coefficient of friction

## Greek letters

$\mu$	Kinematic viscosity ( $\text{mm}^2 \text{s}^{-1}$ )
$\rho$	Density ( $\text{kg m}^{-3}$ )

## Subscripts

e	Entrance
---	----------

nf Nanofluid

bf Base fluid

## 1. Introduction

Tribology is the science of control and handling of wear, friction, and lubrication. Lubrication is a method of preventing friction and abrasion of moving surfaces that lump together. The friction is undesirable in most machines, so it is always attempted to be reduced or eliminated. Friction also causes erosion, noise, reducing durability, and heat generation of the equipment. Loss of energy is the most significant problem caused by wear and friction [1, 2]. Good lubricant quality is required to reduce friction and improve the performance of parts of a machine or surfaces that are in contact with each other. Since most oils cannot be used directly or purely, they are mixed with certain additives to improve their viscosity and properties, most of which are nanomaterials [3-6]. Nanoparticles can enhance the tribological and anti-wear characteristics of oils by one of the following mechanisms (1) rolling effect, which can occur in the presence of small spherical nanoparticles rolling between the two contacting surfaces altering the sliding friction to rolling friction, (2) in the mending effect the mass loss will be compensated due to the incorporation of nanoparticles from the physical film, (3) nanoparticles polish the contact surface and decrease the surface roughness, and (4) nanoparticles protect the contacting surfaces by providing a stable tribo-film [7]. Nano lubricants are mainly used in the turbine meter to reduce friction and wear in bearings. Most turbine meters are equipped with a lubrication system that changes the oil pump's size based on the turbine meter's capacity. Constant lubrication of the turbine meter is required to achieve a longer service life.

Carbon nanotubes (MWCNTs) have attracted attention due to their remarkable properties, such as small size, high surface density, and weak covalent bonds, leading the plates to slip on

each other, reducing the friction of the contact plates in the lubrication system [8-13]. In addition, MWCNTs/nanofluid has excellent physicochemical and heat transfer properties viz. thermal conductivity, high thermal stability, high viscosity index, low pour point, and high flash point [14-23].

Titanium dioxide ( $\text{TiO}_2$ ) nanoparticles are used in many industries because of their excellent heat transfer, lubricity, optical, electrical, and catalytic properties. These applications include industrial pigments, environmental clean-up photocatalysts, skin protectors in sunscreens, and lubricants as additives [24-29]. Many investigations have shown the anti-friction characteristics of  $\text{TiO}_2$  nanoparticles due to their inherent anti-friction functionality, ease of synthesis, and low toxicity [30-33].

Different parameters of nanoparticles such as structure, functional surface groups, and concentrations affect the tribological properties of lubricants. The shape of the nanoparticles is another crucial parameter; the nanospheres experience more pressure at a given load than the nanoparticles because the former contact surface area is much smaller. Therefore, using layer nanoparticles can minimize the deformation of the wear surfaces [34-38]. Studies have shown that even a small concentration of nanoparticles can effectively improve the tribological properties. However, all the operating system parameters must be considered to find the optimum concentration for the minimum coefficient of friction [39-42]. Numerous studies have been conducted to investigate the effect of  $\text{TiO}_2$  nanoparticles and MWCNTs on the tribological properties of base fluid, which in most cases improved the performance of the lubricants and oils [43-50].

Heris et al. [51] investigated the thermal conductivity of turbine oil-based nanofluids inside a circular tube under laminar flow and constant flow rate. Three different nanofluids were prepared using  $\text{TiO}_2$ ,  $\text{CuO}$ , and  $\text{Al}_2\text{O}_3$  nanoparticles at different concentrations. The results showed an increase in heat transfer coefficient and Nusselt number with the addition of

nanoparticles. They also introduced a parameter as the ratio of nanofluid pressure drop to base fluid pressure drop and observed that this parameter was always greater than one. In other words, the addition of nanoparticles increased the pressure drop. Hosseinzadeh et al. [52] evaluated the effect of magnetic field and nanoparticle concentrations on heat transfer coefficient and friction in the presence of water and  $\text{Fe}_3\text{O}_4$  nanoparticles. The experiments were performed inside a horizontal tube with a diameter of 7 mm and a length of 1 meter in different Reynolds numbers. The results showed that the Nusselt number increased with the addition of nanoparticles and Reynolds numbers. Additionally, the same result was observed with increasing magnetic field strength. The presence of nanoparticles increased the coefficient of friction but increasing the intensity of the magnetic field had no significant effect on the coefficient of friction. Furthermore, increasing the Reynolds number decreased the coefficient of friction. Ahmad Ali et al. [53] conducted a study to assess the effect of  $\text{TiO}_2$  and  $\text{Al}_2\text{O}_3$  nanoparticles on the thermophysical and tribological characteristics of engine oil. The outcomes revealed that the coefficient of friction decreased by 40~50% and the tire wear rate decreased by 20~30%. They concluded that adding nanoparticles could remarkably enhance the thermophysical and tribological properties of engine oil. Borda et al. [54] examined the effect of Cu nanoparticles on mineralized and synthesized oil-based esters considering different concentrations. Their findings exhibited that the addition of Cu nanoparticles did not have a good effect on friction and wear on the synthesized oil. However, adding these nanoparticles to mineral oil decreased the coefficient of friction and improved the wear properties, especially at 0.3 wt% of the nanoparticles. Laad et al. [55] added  $\text{TiO}_2$  nanoparticles to improve the lubricating oil properties. Nanofluids were prepared at different concentrations, 0.3, 0.4, and 0.5 wt%. A pin-on-disc tribometer was used to perform abrasion and friction tests. The results showed that the coefficient of friction increased with increasing the nanoparticles concentration. They asserted that the addition of this nanoparticle could reduce the amount of

wear and coefficient of friction and improve the lubricant properties. Curà et al. [56] studied the effect of graphene nanoplates on the tribological performance of lubricants considering different concentrations. It was observed that the addition of the used nanoparticles could significantly improve the tribological features of the lubricants. Hussein et al. [57] experimentally examined the effect of MWCNT/water nanofluids on heat transfer attributes and pressure drop at diverse concentrations ranging from 0.075–0.25 wt%. The experiments were conducted inside a circular mini tube under a laminar flow condition. The results showed that as the nanoparticle concentration increased, the coefficient of friction, the coefficient of heat transfer, and pressure drop increased. A 10% increase in pressure drop was reported at the highest concentration of nanoparticles. The effect of adding MWCNTs and graphene nanoplatelets on the thermal properties of the diesel oil at different concentrations and flow rates were assessed by Naddaf et al. [58]. The outcomes confirmed that the thermal properties of the prepared nanofluids were dependent on the concentration of nanoparticles. They further reported that both the convective heat transfer coefficient and the pressure drop increased with the addition of nanoparticles. Mousavi et al. [59] investigated the thermophysical and rheological properties of MoS<sub>2</sub>/diesel oil-based nano lubricants. A pin-on-disc friction and wear tester was employed to evaluate the friction and anti-wear properties. The highest viscosity and viscosity index were observed at the highest concentration in the study, 0.7 wt%. Ajeel et al. [60] evaluated the simultaneous effect of corrugated walls and turbulent flow of nanofluids on thermohydraulic performance. The experiments were conducted at diverse Reynolds numbers ranging in 10,000–30,000 and a heat flux of  $10000 \frac{W}{m^2 K}$ . Three different channel shapes were considered as a semicircular, wavy channel, trapezoidal wavy channel, and straight channel. The nanofluids were prepared in volumetric percentages of 1% and 2% of Al<sub>2</sub>O<sub>3</sub>. The results showed that the nanofluid flow inside the trapezoidal corrugated channel increased 63.54% of the heat transfer coefficient and 1.37 times the pressure drop compared to

the straight channel. Pourpasha et al. [61] assessed the effect of CNT on the thermophysical and tribological features of turbine oil meter nano lubricants. The thermophysical properties of lubricating oil such as viscosity index, kinematic viscosity, flash point, pressure drop, and coefficient of friction were measured. It was found that the addition of CNT could enhance lubrication characteristics and improve the thermophysical of the turbine meter oil nano lubricants.

Based on the performed literature survey, most studies in the field of heat transfer characteristics of nano lubricants announce a positive effect on the friction-reduction behavior and thermophysical characteristics considering different nano additives. However, in the previous investigations, none of the studies were conducted while considering  $\text{TiO}_2$  and MWCNTs nanoparticles in the turbine meter oil. Furthermore, heat transfer characteristics and tribological behaviors of the  $\text{TiO}_2$  and MWCNTs nano lubricants have not been well-understood. It is worth mentioning that different effective parameters such as concentration of nanoparticles, flow rates, and pressure drops were comprehensively studied in this study.

In this study, to the best of our knowledge, lubrication oil simulation has been measured inside the turbine for the first time. The velocity profiles, pressure drop values, coefficient of friction of the base fluid, and nano lubricants considering MWCNTs and  $\text{TiO}_2$  nanoparticles considering different weight percentages and volume flow rates were comprehensively investigated.

## **2. Experimental Section**

### **2.1. Materials**

Table 1 lists the specifications of the gas turbine meter oil manufactured by Shell Oil Company, USA. The  $\text{TiO}_2$  and MWCNTs were commercially purchased from SkySpring Nanomaterials, USA, and US Research Nanomaterials, USA, respectively. These data were



reported by Pourpasha et al. [61]. Table 2 represents the specifications of the used nanomaterials. Figures 1 and 2 represent the SEM images of TiO<sub>2</sub> nanoparticles and MWCNTs, respectively. The specification of nanofluids is listed in Table 3.

**Table 1** Specifications of gas turbine meter oil.

Properties	Unit	ASTM standard	Value
Density	Kg/m <sup>3</sup>	D1298	775
Viscosity at 40°C	cSt	D445	21.88
Viscosity at 100°C	cSt	D445	4.6
Viscosity index (VI)	—	D2270	130
Pour point	°C	D97	−40
Flash point	°C	D92	220

**Table 2** Physical properties of nanoparticles.

Nanoparticles	Morphology	Purity (%)	Average diameter (nm)	Density (kg/m <sup>3</sup> )	Color
TiO <sub>2</sub>	Spherical	99.5	10	4230	White
MWCNTs	Cylindrical	>95	13	2100	Black/Gray

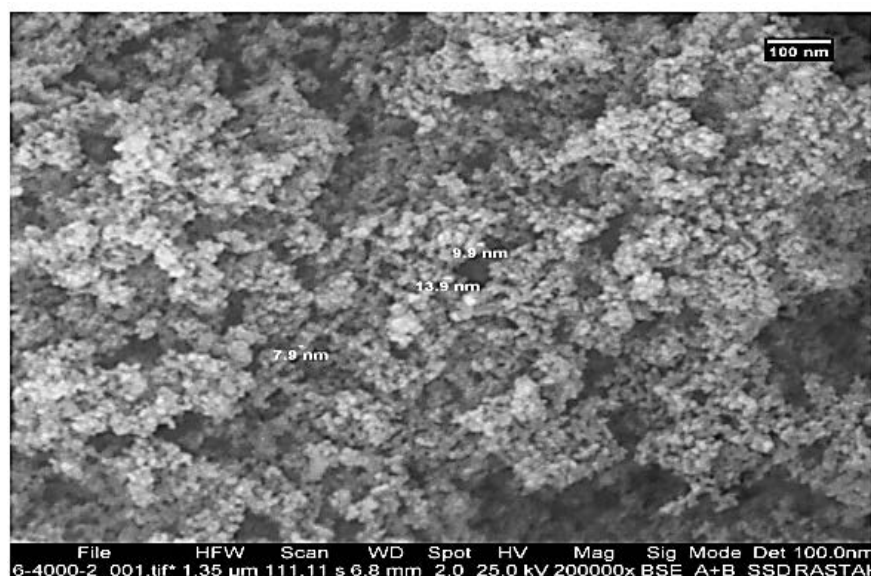


**Fig. 1.** SEM image of TiO<sub>2</sub> nanoparticles.

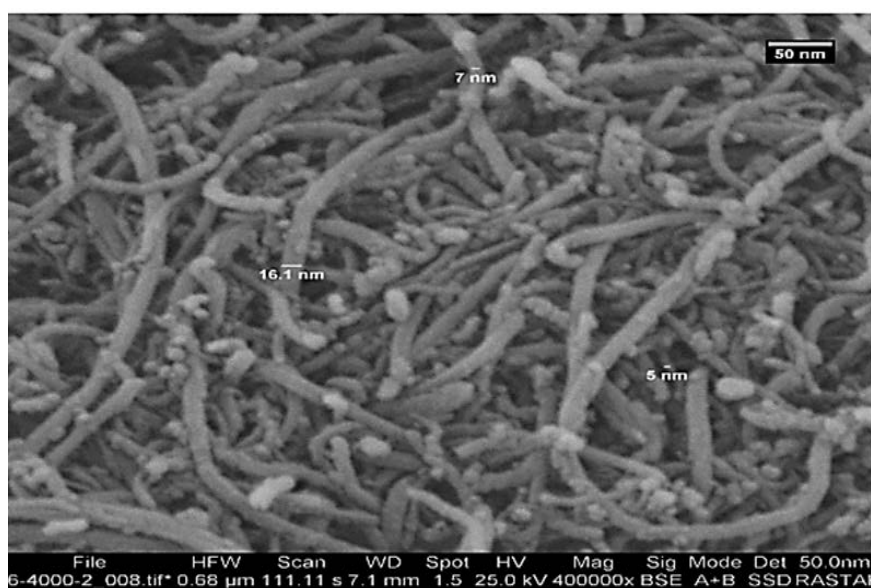


**Fig. 2.** SEM image of MWCNTs.

**Table 3** Specifications of nanofluids.

Nanofluid	Density (kg/m <sup>3</sup> )	Viscosity at 40°C (cSt)
0 (Base oil)	775	21.88
0.1 wt% TiO <sub>2</sub>	776	21.407
0.2 wt% TiO <sub>2</sub>	776.4	21.645
0.3 wt% TiO <sub>2</sub>	777	21.826
0.1 wt% MWCNTs	775.8	21.651
0.2 wt% MWCNTs	776.4	21.852
0.3 wt% MWCNTs	777	22.071

## 184 2.2. Methods for experiment

185 The velocity inlet is essential information needed for modeling nanofluid flow through the  
 186 gas turbine meter conduit. The oil pathway and the pump were used to measure the velocity.  
 187 Figure 3 shows the oil inlet pathway for the velocity measurement system. A certain amount  
 188 of oil was pumped through the oil pump to the oil pathway to measure inlet velocity. The inlet  
 189 velocity was determined by measuring the time to complete oil outflow using equation 1.

$$Q = U \times A \quad (1)$$

190 where  $Q$  is the volume flow rate (m<sup>3</sup>/s),  $U$  is the velocity (m/s), and  $A$  is the cross-sectional  
 191 area (m<sup>2</sup>).



**Fig. 3.** Turbine meter oil inlet pathway for the velocity measurement system.

### 2.3. The pressure drops from theoretical relationships

Two types of energy loss for pipes can be considered: first is the loss due to the change in the diameter of the pipes and the types of joints (minor loss). Second is the loss due to friction in the pipes (major loss), higher than the other. Factors such as changing the diameter of the pipes and the existence of different types of joints (knees, valves, and curvature in the pipes.) cause the deformation of the flow lines resulting in energy loss. The following formula can calculate this type of loss [62]:

$$h_f = K \frac{U^2}{g} \quad (2)$$

$$\Delta P = \rho g h_f \quad (3)$$

In the above relation,  $K$  is the local energy dissipation coefficient (the empirical coefficient obtained from the corresponding tables without dimension),  $U$  is the velocity (m/s) (the inlet

203 velocity),  $\Delta P$  is the pressure drop (Pa),  $\rho$  as density ( $kg/m^3$ ), and  $g$  is the gravitational  
204 acceleration ( $m^2/s$ ).

205 Depending on the shape and geometry, this type of pressure loss involves a pressure drop  
206 caused by the presence of a knee and a sudden change in the cross-sectional area. The  
207 coefficient of local energy loss resulting from the cross-sectional area change can be obtained  
208 from equation 4 [63]:

$$K = \left(1 - \frac{A_1}{A_2}\right)^2 \quad (4)$$

209 where  $A_1$  is a small cross-section and  $A_2$  is a large cross-section.

210 The simulation has been performed at a constant temperature without heat transfer, steady-  
211 state condition, and under the laminar flow condition. The frictional pressure drop is dependent  
212 on the friction between the fluid and the pipe, which is shown for a circular pipe with the  
213 Darcy-Weisbach relation.

$$\Delta P = F_D \times \frac{\rho L}{2} \times \frac{U^2}{D} \quad (5)$$

$$F_D = \frac{64}{Re} \quad (6)$$

$$Re = \frac{\rho U D}{\mu} \quad (7)$$

214 Where  $\Delta P$  is pressure drop [Pa],  $F_D$  is coefficient of friction,  $D$  is diameter [m],  $L$  length of  
215 pipe [m],  $\rho$  is density [ $Kg/m^3$ ],  $U$  is velocity [m/s], and  $\mu$  is viscosity [kg/m.s].

## 216 **2.4. Developing entrance length and developed flow and theoretical relationships**

217 For laminar flow, the hydrodynamic entrance length can be obtained from the following  
218 equation [64]:

$$\frac{l_e}{D} = 0.058 Re \quad (8)$$

where  $l_e$  is the entrance length and  $D$  is the diameter of the pipe.

### 3. Numerical simulation

#### 3.1. Simulation of nanofluids

As mentioned, this study aims to simulate the flow of nanofluids inside the oil pathway. Single-phase and general two-phase methods are used to model the flows involving nanoparticles. In the two-phase approach, nanofluids are considered two different liquid and solid phases with different momentums. The equations resulting from the two-phase theory are difficult to deal with and cannot be easily applied for nanofluids. In the single-phase approach, both the fluid phase and nanoparticles are considered a single homogeneous phase. Since the particles are ultrafine and become easily fluidized, all the equations of continuity, motion, and energy for pure fluid may be directly extended to nanofluids. In this study, due to the low concentration of nanoparticles and the experimental determination of properties such as viscosity and density, the homogeneous model has been used to simulate the nanofluid flow through the gas-turbine oil meter path.

#### 3.2. Governing Equations

The pressure drop is obtained from the continuity and momentum balance equations. Equations 5, 7, and 8 represent these equations.

$$\frac{\partial \rho}{\partial t} + \nabla \cdot (\rho \vec{v}) = 0 \quad (7)$$

$$\frac{\partial}{\partial t} (\rho \vec{v}) + \nabla \cdot (\rho \vec{v} \vec{v}) = -\nabla P + \nabla \tau + \rho \vec{g} + \vec{F} \quad (8)$$

$$\frac{\Delta P}{L} = F_D * \frac{\rho}{2} * \frac{V^2}{D} \quad (9)$$

where  $P$  is the static pressure,  $\Delta P$  is a pressure drop,  $\rho \vec{g}$  and  $\vec{F}$  are the gravitational body force and exterior body forces,  $F_D$  is coefficient of friction, and  $D$  is diameter [63].

In the homogeneous model, the thermophysical properties of nanofluid such as viscosity and density must be used in continuity, momentum, and energy equations.

In the present study, experimental values of viscosity and density are given by Pourpasha et al. [61] were used in the continuity and momentum equations.

### 3.3. Boundary conditions and needed information

The purpose of this present study is to investigate the effect of MWCNTs and  $\text{TiO}_2$  nanoparticles on the modeling of lubricant fluid flow within gas turbine meters. A lubrication system is necessary due to the high degree of wear and coefficient of friction of the bearings. In this regard, the lubricating oil pathway inside the gas turbine meters has been investigated and simulated. The CMM scanner scans the oil path in figure 4.. The condition used as the boundary condition is the inlet velocity is 0.00483, 0.0409, and 0.012 ( $m/s$ ). The dimension of the oil pathway is shown in figure 5. The oil pathway from part 1 to part 4 is iron, and part 5 is steel. The simulation is performed at a constant temperature without heat transfer, steady-state condition, and under the laminar flow condition.

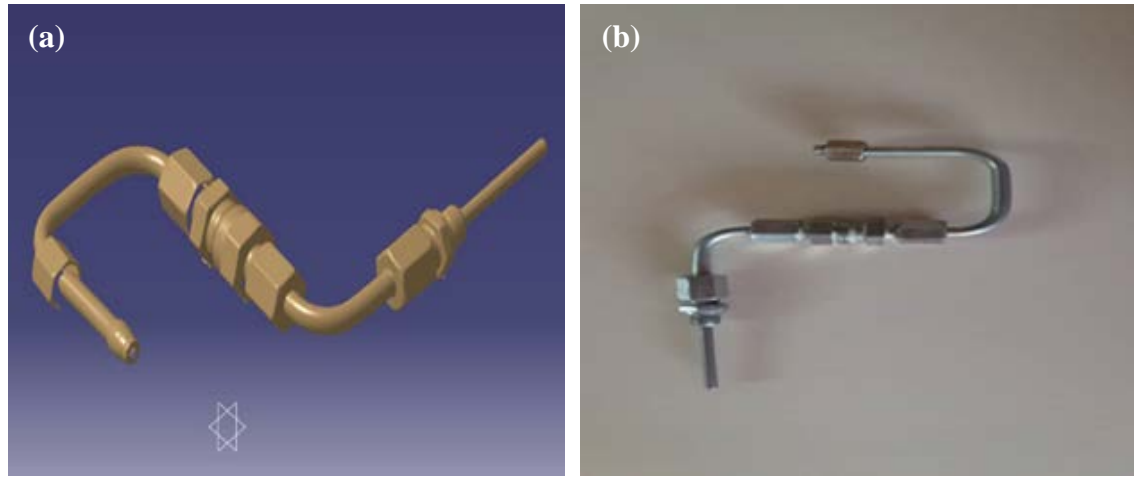


**Fig. 4.** (a) Scanned and (b) the real photo of the turbine meter oil pathway.

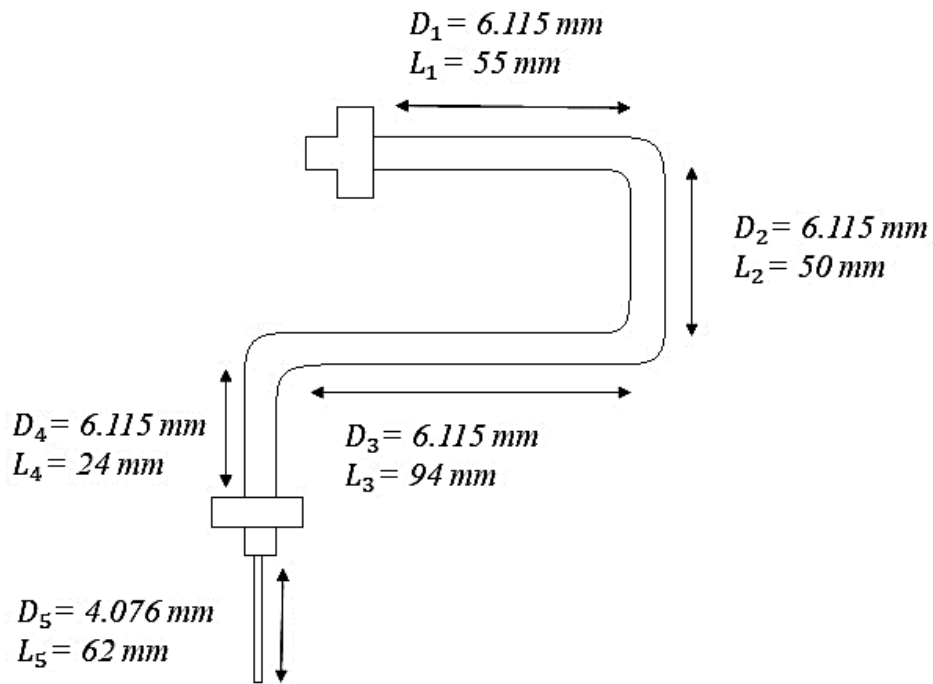


**Fig. 5.** Dimension of oil pathway.

### 3.4. Numerical Analysis

The oil pathway is meshed by Gambit software version 2. 4. 6 and the equations have been solved by Fluent software version 19.1. ANSYS-FLUENT software has been used to solve the



governing equations discretized with a double-precision solver using the SIMPLEC algorithm. The convergence criteria for continuity, momentum, and energy equations were all set to  $10^{-6}$ .

For the mesh independence check, figure 6 is plotted, and given the optimal number of cells, 368462 is selected. The absolute convergence criteria for the continuum equation and the velocity equation with residuals below have been considered.

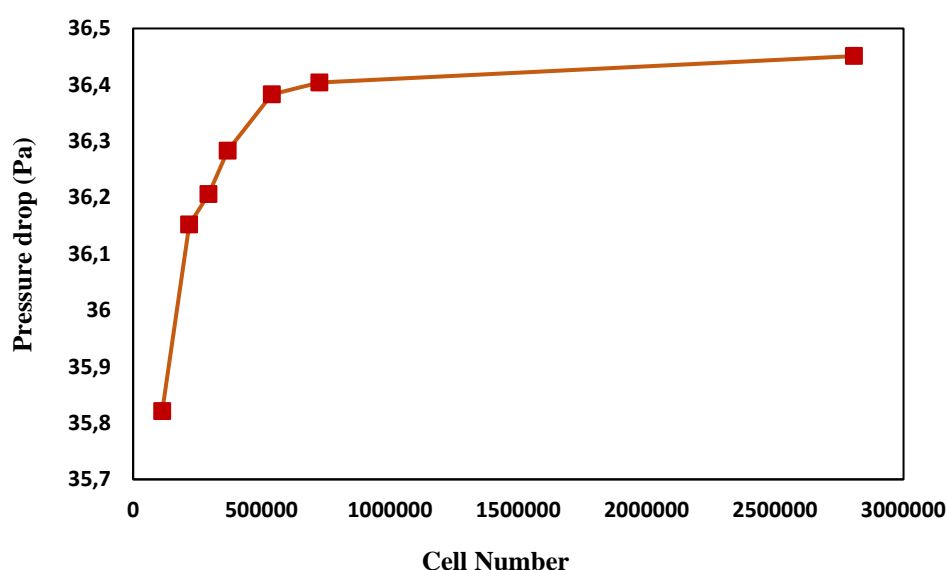


**Fig. 6.** Pressure drop variations versus cell number.

## 4. Results

### 4.1. Results of TiO<sub>2</sub>/turbine meter oil nanofluids

This section discusses the effect of increasing volume flow rate and mass percent of nanoparticles on pressure drop, coefficient of friction, and velocity profile. Furthermore, the effect of simultaneous mass percent of nanoparticles and volume flow rate on pressure drop and coefficient of friction are discussed. Different results are presented in Table 4 to compare the outlet velocity of the simulation and the theoretical relationships. The differences between experimental and numerical values of outlet velocities are 2.48%, emphasizing the accuracy

275 and correctness of the numerical simulation. Table 5 lists the pressure drop values of  
 276 TiO<sub>2</sub>/turbine meter oil nanofluid at volume flow rates of 0.14, 0.35, and 1.2  $\frac{cm^3}{s}$ . Figure 7 shows  
 277 the effect of TiO<sub>2</sub> concentration on the pressure drop variations as a function of flow rate.

278 **Table 4** The velocity values of modeling and theoretical relationships.

Fluid	Inlet velocity (m/s)	Modeling outlet velocity (m/s)	Theoretical outlet velocity (m/s)	Difference (%)
Base oil	0.00483	0.0106	0.01087	2.48

279

280 **Table 5** Modeling and theoretical pressure drop values of TiO<sub>2</sub> nanofluids at different flow rates.

Concentration (wt%)	Flow rate ( $\frac{cm^3}{s}$ )	Modeling pressure drop (Pa)	Theoretical pressure drop (Pa)	Difference (%)
0 (base oil)	0.14	36.28	36.44	0.439
	0.35	90.59	90.64	0.055
	1.2	314.91	310.74	1.342
0.1 TiO <sub>2</sub>	0.14	36.73	36.90	0.461
	0.35	91.68	92.60	0.994
	1.2	318.65	313.17	1.750
0.2 TiO <sub>2</sub>	0.14	37.15	37.31	0.429
	0.35	92.72	93.08	0.387
	1.2	322.20	316.80	1.705
0.3 TiO <sub>2</sub>	0.14	37.50	37.67	0.451
	0.35	93.60	93.62	0.021
	1.2	325.19	319.81	1.682

281

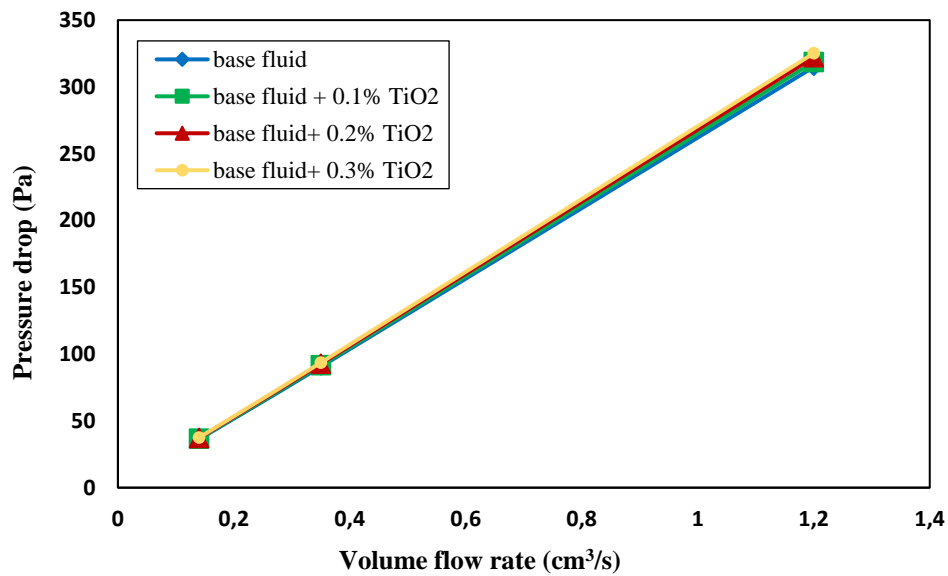


**Fig. 7.** The effect of TiO<sub>2</sub> concentration on the pressure drop variations as a function of flow rate.

The maximum difference between the values of the pressure drop obtained from the simulation and the theoretical pressure drop is 1.75%, indicating acceptable accuracy of the simulation. According to figure 7 and Table 5, it can be seen that by increasing the concentration of TiO<sub>2</sub> nanoparticles at a given volume flow rate, the pressure drop increased due to the increased viscosity. As the concentration of the nanoparticles increases, the interaction between the nanoparticles increases, which also increases the viscosity. According to equation 5, the increment of viscosity can lead to an increase in pressure drop. To illustrate, by increasing the concentration from 0.1 to 0.3 wt% at a flow rate of  $1.2 \frac{\text{cm}^3}{\text{s}}$ , the pressure drop reached 318.65 Pa from 325.19 Pa. The higher the flow rates and the concentrations, the more pressure drop. The reason for this variation can be due to the insignificant change in viscosity at lower concentrations since nanoparticles could not affect the viscosity. Other scholars have indicated similar results in the experimental investigation [57, 58].

Figure 8 exhibits pressure drop variation of TiO<sub>2</sub> nanofluids at different volume flow rates. According to figure 8 and Table 5, it can be seen that as the flow rate increased, pressure drop increased for all concentrations, as it is followed by the fluid velocity increase and the direct

relationship of pressure drop with fluid velocity (equation 5). Additionally, considering equation 7, the Reynolds number is related to tube length, velocity, viscosity, and nanofluid density. Given the constant length of the tube and minor changes in viscosity and density, the leading cause of the pressure drop is related to an increase in flow rate. The highest pressure drop rate at any given concentration is related to the highest flow rate. For instance, by increasing the volume flow rate from 0.14 to  $1.2 \frac{\text{cm}^3}{\text{s}}$ , the pressure drop increased from 36.34 Pa to 318.65 Pa for 0.1 wt%  $\text{TiO}_2$  nanofluid; thus, the volume flow rate has a significant effect on the pressure drop. In a study conducted by Mousavi et al. [59], the pressure drop variations of the prepared nanofluids in a tube were investigated. Their findings were consistent with the modeling results.

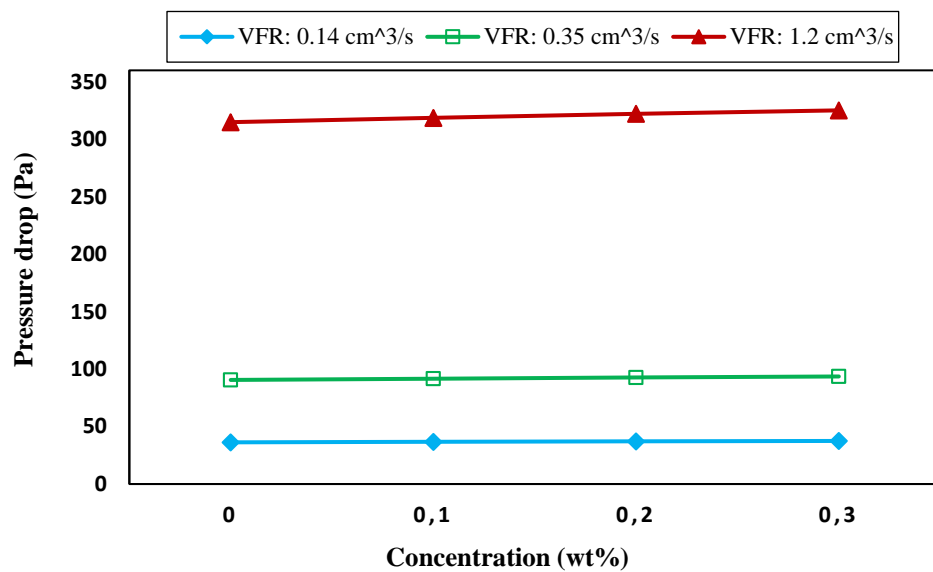


**Fig. 8.** Pressure drop variation of  $\text{TiO}_2$  nanofluids at different volume flow rates.

Figure 9 represents the effect of volume flow rate on the pressure drop ratio of  $\text{TiO}_2$  nanofluids and pure oil. It can be seen that the increase in the volume flow rate of all prepared  $\text{TiO}_2$  nanofluids led to a decrease in the pressure drop of the nanofluid to the base fluid. As the settling probability decreases; there will be a reduction in the high-volume flow rate, the ratio

of nanofluid pressure drop to base fluid pressure drop. By increasing the flow rate at the same concentration, the number of nanoparticles per volume was reduced, leading to a decrease in apparent viscosity. Also, this pressure drop ratio intensified with an increase in the concentration of nanoparticles at given volume flow rates. Pourfarhang et al. [65] studied the nanofluid flowing inside a car radiator and found that with increasing flow, the ratio of pressure drop to the base fluid decreases, and this result is consistent with the outputs of the simulation.

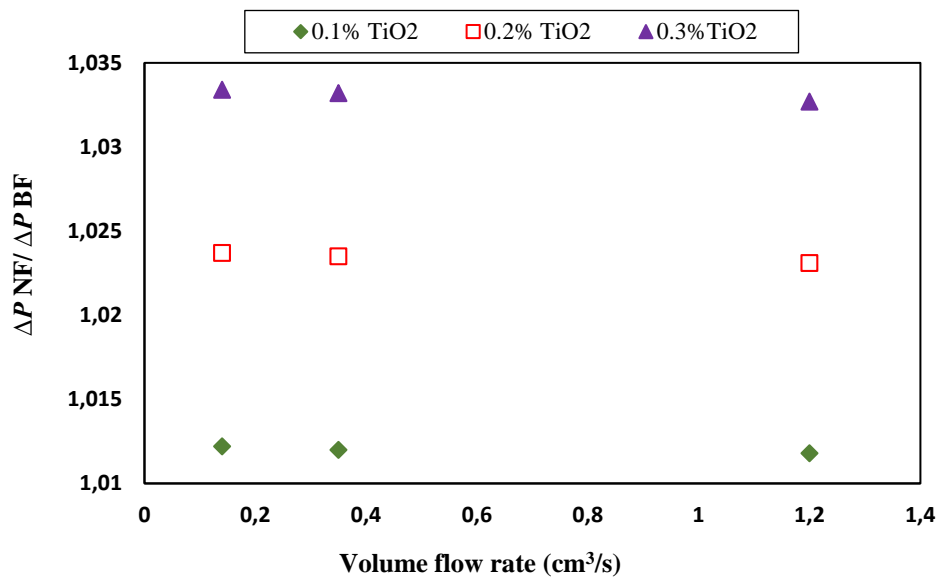


**Fig. 9.** Pressure drop ratio of TiO<sub>2</sub> nanofluids to base oil at different flow rates.

To investigate the coefficient of friction variations (Darcy's Weisbach coefficient of friction), the coefficient of friction of a pipe with a larger diameter was called  $F_1$ . The coefficient of friction of a pipe with a smaller diameter was called  $F_2$ . Table 6 is provided to compare the changes made on the coefficient of friction. Based on Table 6, the increase in the concentration of nanoparticles led to an increase in the coefficient of friction. At higher concentrations, the viscosity of the fluid and the coefficient of friction increased due to the agglomeration of nanoparticles. It is also apparent that as the volume flow rate increases, the coefficient of friction decreases since the coefficient of friction is inversely related to the fluid

velocity (Eq. 5). Many researchers have also found that the coefficient of friction increases with the increasing concentration of nanoparticles and decreases with the increasing flow rate [1, 2, 59, 66].

**Table 6** Coefficient of friction at different concentrations and velocities of TiO<sub>2</sub> nanofluids.

Concentration (wt%)	Inlet velocity (m/s)	$F_1$	$F_2$
0 (base oil)	0.00483	45.88	31.37
	0.012	18.47	12.64
	0.0409	5.42	3.61
0.1 TiO <sub>2</sub>	0.00483	46.38	31.90
	0.012	18.67	12.78
	0.0409	5.48	3.78
0.2 TiO <sub>2</sub>	0.00483	46.89	32.00
	0.012	18.87	12.92
	0.0409	5.54	3.80
0.3 TiO <sub>2</sub>	0.00483	47.30	32.32
	0.012	19.04	13.03
	0.0409	5.59	3.83

Figure 10 shows the effect of adding TiO<sub>2</sub> nanoparticles on the velocity profile and reaching the fully developed state. It shows the state of the velocity profile at the tube's inlet for the base fluid and nanofluids containing 0.1, 0.2, and 0.3 wt% of TiO<sub>2</sub> nanoparticles at a volume flow rate of  $0.14 \frac{cm^3}{s}$ . In addition, with the addition of TiO<sub>2</sub> nanoparticles and increasing the concentration of nanoparticles, reaching the developed state occurs faster. Adding TiO<sub>2</sub> nanoparticles led to an increase in viscosity; thus, considering equations 7 and 8, Reynolds

number and the entrance length decreased, and reaching the fully developed state occurred faster.

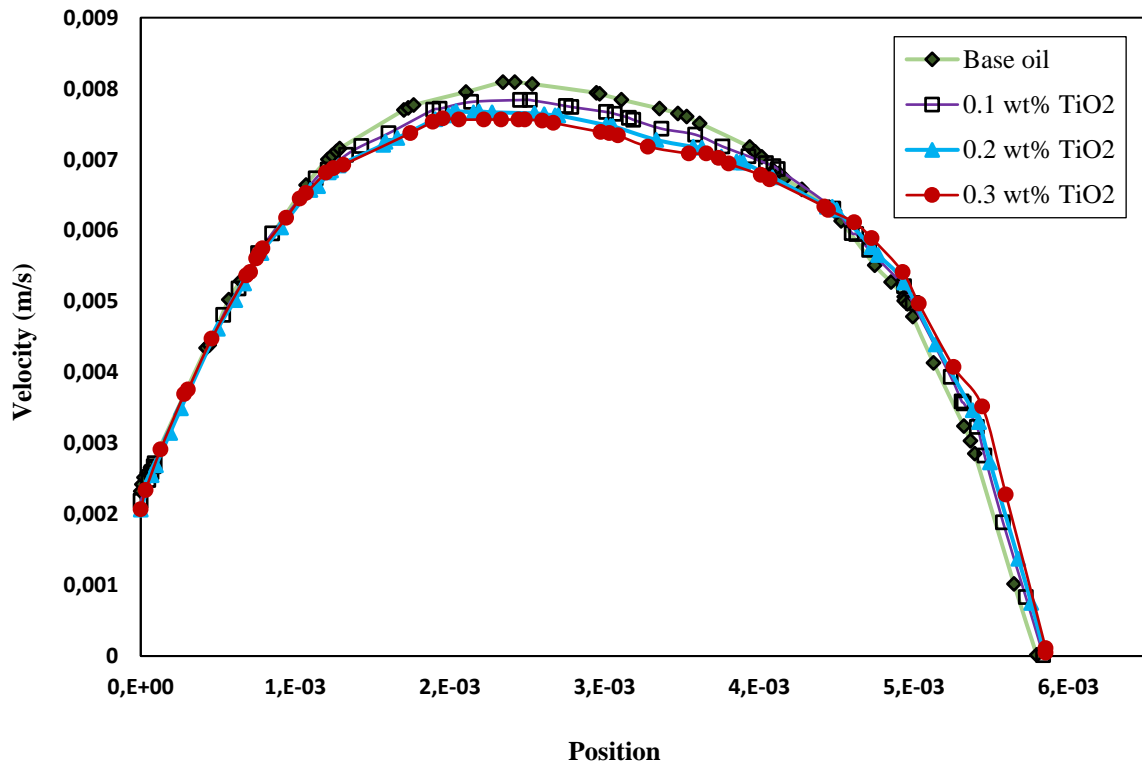


**Fig. 10.** Velocity profile of TiO<sub>2</sub> nanofluids at pipe inlet at a volume flow rate of  $0.14 \left(\frac{\text{cm}^3}{\text{s}}\right)$  and different concentrations.

Figure 11 exhibits the effect of volume flow rate of 0.2 wt% TiO<sub>2</sub> nanofluid on the velocity profile. It shows the velocity profile status at the inlet of the pipe containing 0.2 wt% of TiO<sub>2</sub> nanoparticles at different volume flow rates. It is observed that the increase of flow rate can delay reaching the developed state. Because with increasing flow, the velocity increases, and according to Equation 7, the Reynolds number increases. According to Equation 8, with increasing Reynolds number, the entrance length increases, and reaching the fully developed state is delayed. Gholinia et al. [67] examined the nanofluid flow inside a circular cylinder and observed that increasing the velocity caused the development state to be delayed.

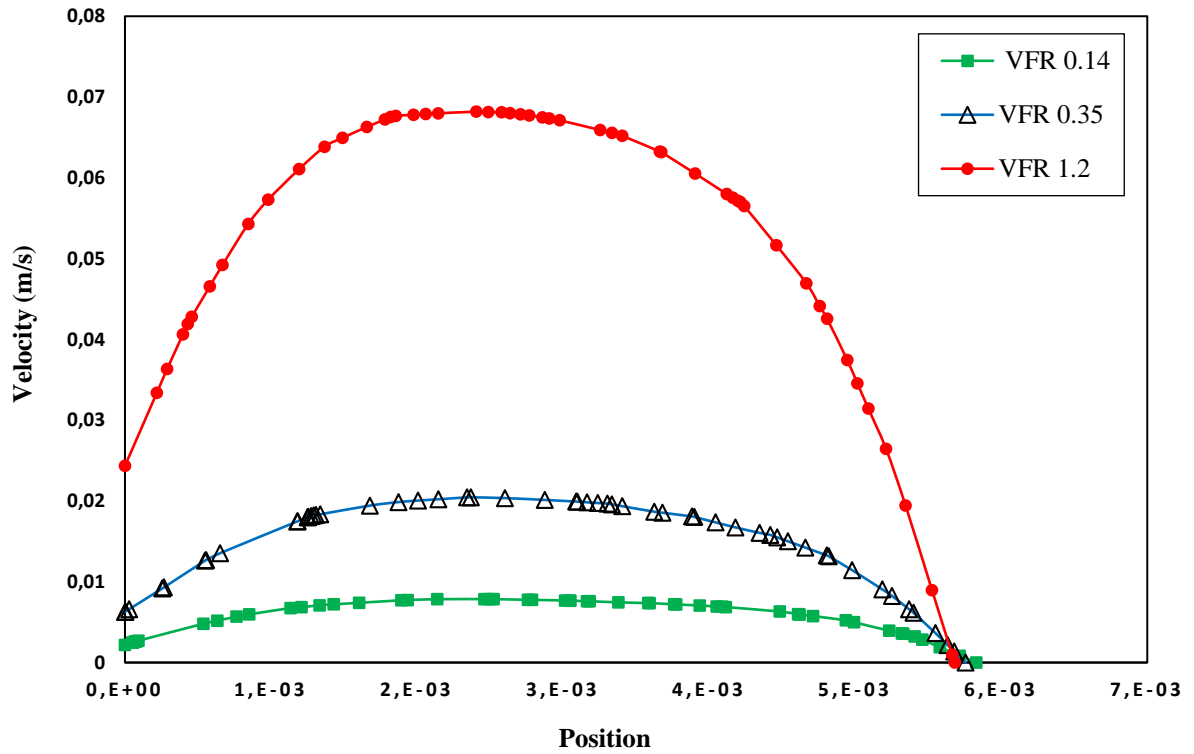


**Fig. 11.** Velocity profile of 0.2 wt%  $\text{TiO}_2$  nanofluids at pipe inlet considering different volume flow rates.

#### 4.2. Results of MWCNTs/turbine meter oil nanofluid

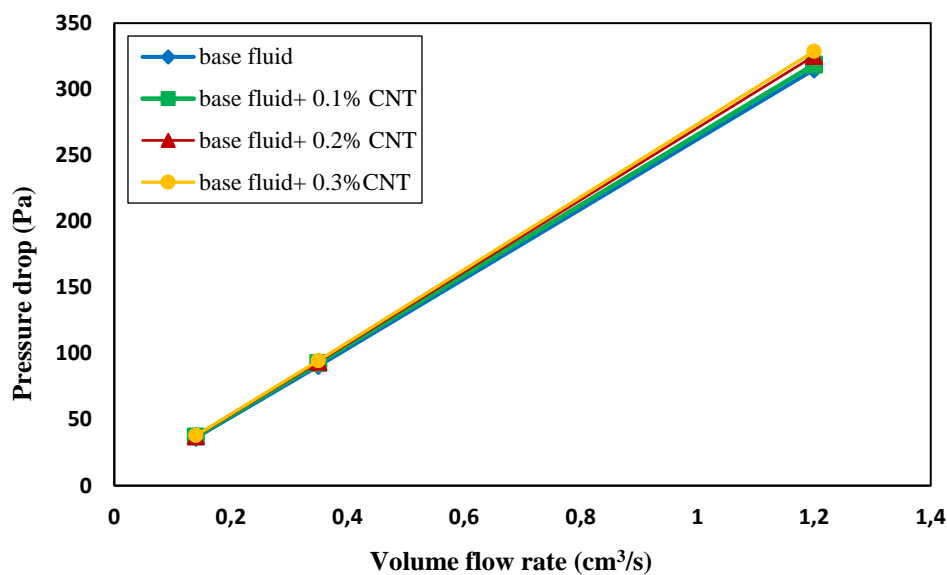
The effect of increasing the concentration of MWCNTs and volume flow rate on pressure drop, coefficient of friction, and velocity profile are discussed in this section. Moreover, the simultaneous effect of increasing the concentration of nanoparticles and volume flow rate on pressure drop are scrutinized.

Table 7 lists the pressure drop values of MWCNTs nanofluids at different volume flow rates. Figure 12 shows the effect of MWCNTs concentration on the variations of the pressure drop as a function of flow rate.



366 **Table 7** Modeling and theoretical pressure drop values of MWCNTs nanofluids at different flow  
367 rates.

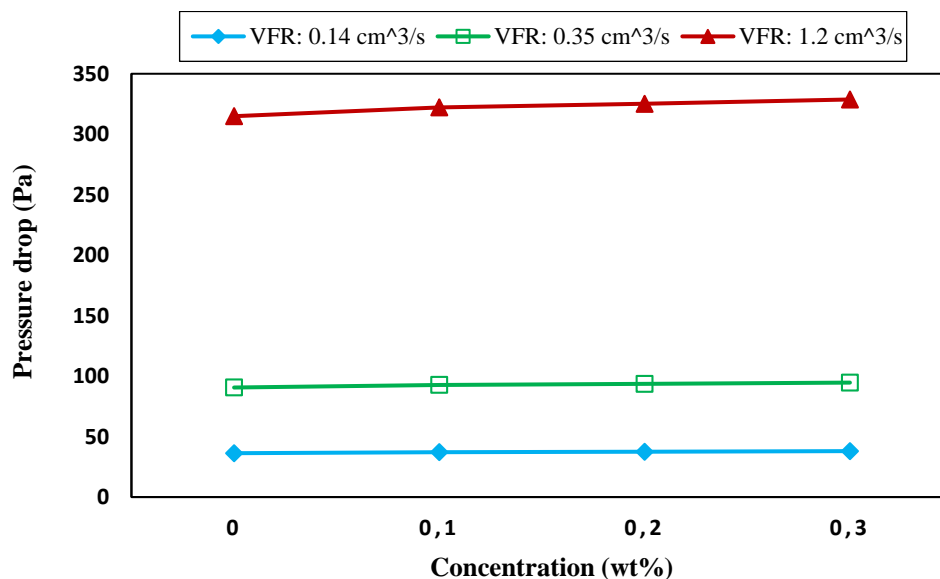
Concentration (wt%)	Flow rate ( $\frac{cm^3}{s}$ )	Modeling pressure drop (Pa)	Theoretical pressure drop (Pa)	Difference (%)
0 (base oil)	0.14	36.28	36.44	0.439
	0.35	90.59	90.64	0.055
	1.2	314.91	310.74	1.342
0.1 MWCNTs	0.14	37.14	37.32	0.482
	0.35	92.72	92.80	0.086
	1.2	322.19	318.63	1.117
0.2 MWCNTs	0.14	37.47	37.68	0.557
	0.35	93.60	93.69	0.096
	1.2	325.18	319.81	1.679
0.3 MWCNTs	0.14	38.00	38.18	0.471
	0.35	94.64	94.65	0.010
	1.2	328.73	323.41	1.645



368  
369 **Fig. 12.** The effect of MWCNTs concentration on the pressure drop variations as a function of  
370 flow rate.

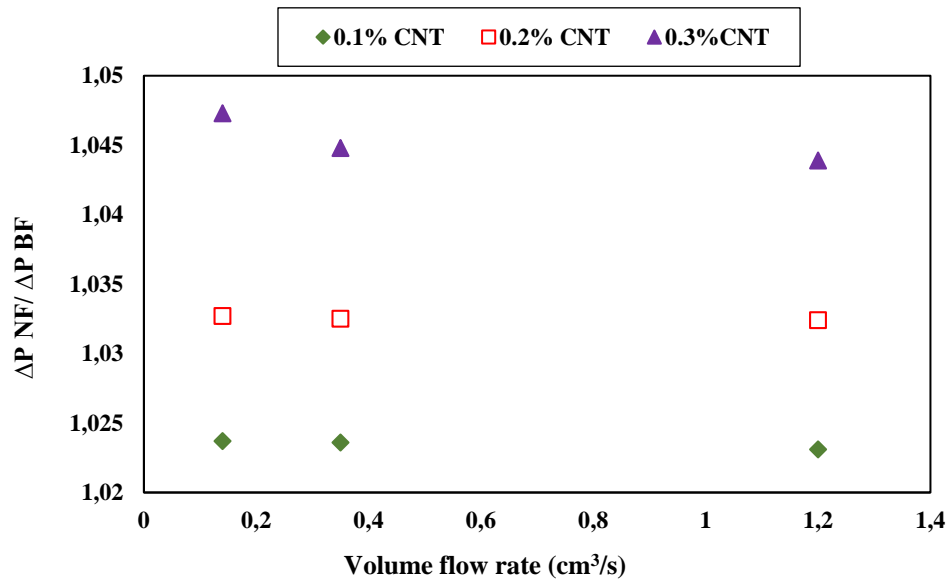
According to Figure 12 and Table 7, the pressure drop of the nanofluid can be increased by increasing the concentration of MWCNTs at a given volume flow rate. The main reason for the increased viscosity is that as the concentration of MWCNTs increases, the collision between the MWCNTs increases because of increased random motion and increases viscosity. Due to the direct relationship of pressure drop with a viscosity (Eq. 5), pressure drop at higher percentages of MWCNTs shows a higher increase. At low concentrations of MWCNTs, the upward pressure drop of nanofluid is much lower than that of high nanofluid concentrations. In other words, at a low concentration of MWCNTs, the increase in pressure drop is not very noticeable due to the unremarkable change in viscosity of nanofluids at low concentrations.

Figure 13 shows pressure drop variation of MWCNTs nanofluids at different volume flow rates. According to Figure 13 and Table 7, it can be concluded that by increasing the volume flow rate, the pressure drop increases, since the increase in volume flow rate results in an increase in fluid velocity and the direct relationship between pressure drop and fluid velocity (Eq. 5). To illustrate, at a 0.3 wt% concentration of MWCNTs, the pressure drop was raised from 38 Pa to 94.64 Pa and then to 328.78 Pa. The results show the significant effect of increasing discharge on increasing pressure drop. In a study conducted by Hussein et al. [57] on a current-carrying nanofluid in a circular – mini - tube, they observed that with increasing flow rate, the pressure drop increased, which was quite similar to the simulation results.



**Fig. 13.** Pressure drop variation of MWCNTs nanofluids at different volume flow rates.

Figure 14 exhibits the effect of volume flow rate and concentration of MWCNTs on pressure drop. It can be seen that by increasing the volume flow rate at all concentrations, the pressure drop of nanofluids to the base fluids decreased. As the volume flow rate increased, the rate of fluid coalescence increased, and the fluid dispersion became uniform. Since nanoparticles' effect was the least at the lowest concentration, nanofluid properties were close to base fluid properties, and the lowest proportion of pressure drop could be seen at the lowest nanoparticle concentration and the highest volume flow rates. Moreover, the probability of sedimentation decreases with the trend. As a result of the high-volume flow rate, the pressure drop rate relative to the base fluid decreased. Therefore, using nanofluids in high volume flow rates will cause less pressure drop and be more appropriate. In the research of Pourfarhang et al. [65] and Naddaf et al. [58], it was observed that the pressure drop ratio of nanofluid to the base fluid decreased with increasing flow rate.



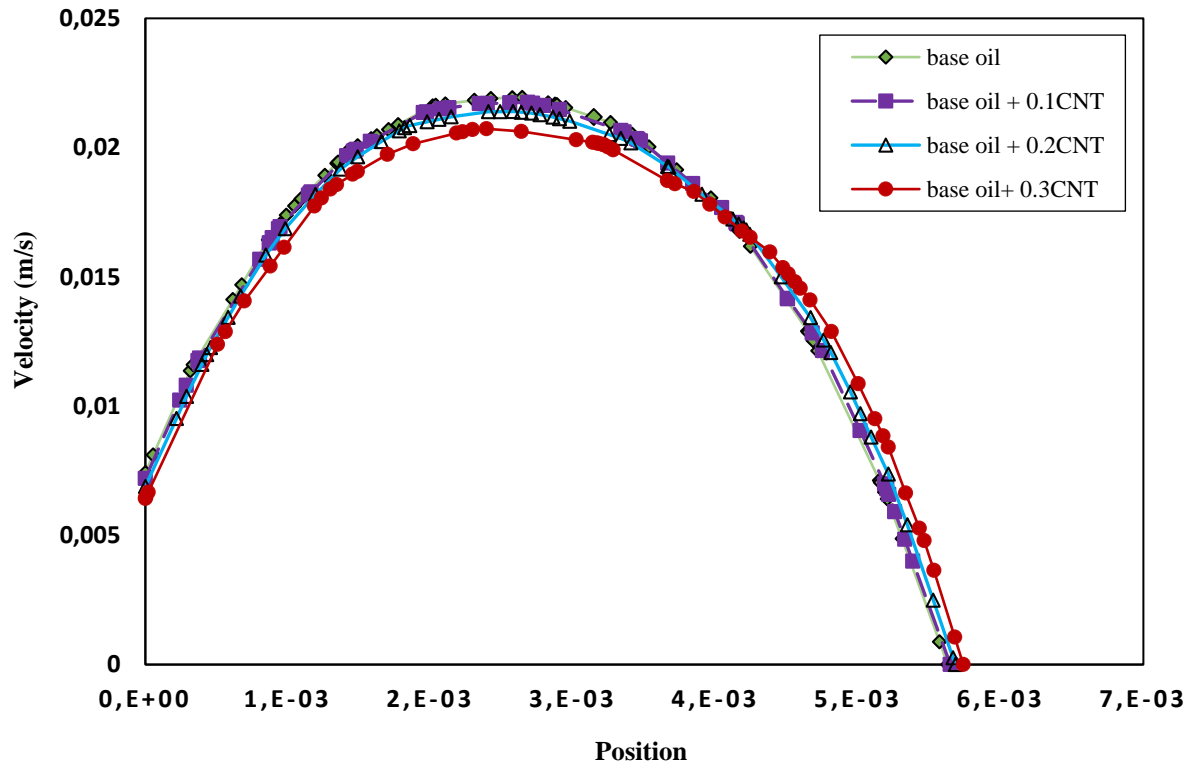
**Fig. 14.** Pressure drop ratio of MWCNTs nanofluids to base oil at different flow rates.

Table 8 lists the coefficient of frictions at different concentrations of MWCNTs nanofluids. Considering Table 8, as the concentration of MWCNTs increased, the coefficient of friction increased. It is also apparent that as the volume flow rate increased, the coefficient of friction decreased because the coefficient of friction is inversely related to the fluid velocity (Eq. 5).

Figure 15 presents the effect of adding MWCNTs on the velocity profile and reaching the fully developed state. It shows the status of the velocity profile at tube inlet for base fluid and nanofluids containing 0.1, 0.2, and 0.3 wt% of MWCNTs at a volume flow rate of  $0.35 \frac{\text{cm}^3}{\text{s}}$ . As can be seen, with the addition of MWCNTs and increasing the concentration of MWCNTs, reaching the developed state can be faster. The Reynolds number decreased with the addition of MWCNTs since they could increase the viscosity. According to Equation 8, with decreasing Reynold number, the entrance length decreases and reaches the fully developed state. The same experimental results were reported in a study conducted by Bao et al. [68].

**Table 8** Coefficient of friction at different concentrations and velocities of MWCNTs nanofluids.

Concentration (wt%)	Inlet velocity (m/s)	$F_1$	$F_2$
0 (base oil)	0.00483	45.88	31.37
	0.012	18.47	12.64
	0.0409	5.42	3.61
0.1 MWCNTs	0.00483	46.96	32.08
	0.012	18.89	12.78
	0.0409	5.54	3.80
0.2 MWCNTs	0.00483	47.34	32.36
	0.012	19.05	12.93
	0.0409	5.59	3.83
0.3 MWCNTs	0.00483	47.83	32.70
	0.012	19.25	13.18
	0.0409	5.65	3.87



**Fig. 15.** Velocity profile at pipe inlet at a volume flow rate of  $0.35 \left( \frac{\text{cm}^3}{\text{s}} \right)$  and different concentrations of MWCNTs.

Figure 16 shows the variations of the velocity profile at the inlet of the tube for nanofluids containing 0.1, 0.2, and 0.3 wt% of MWCNTs at a volume flow rate of  $0.35 \frac{\text{cm}^3}{\text{s}}$ . Increasing flow rate can delay the developed state because the velocity increases, and according to Equation 7, the Reynolds number increases. According to Equation 8, with increasing Reynolds number, the entrance length increases, and reaching the developed state is delayed.

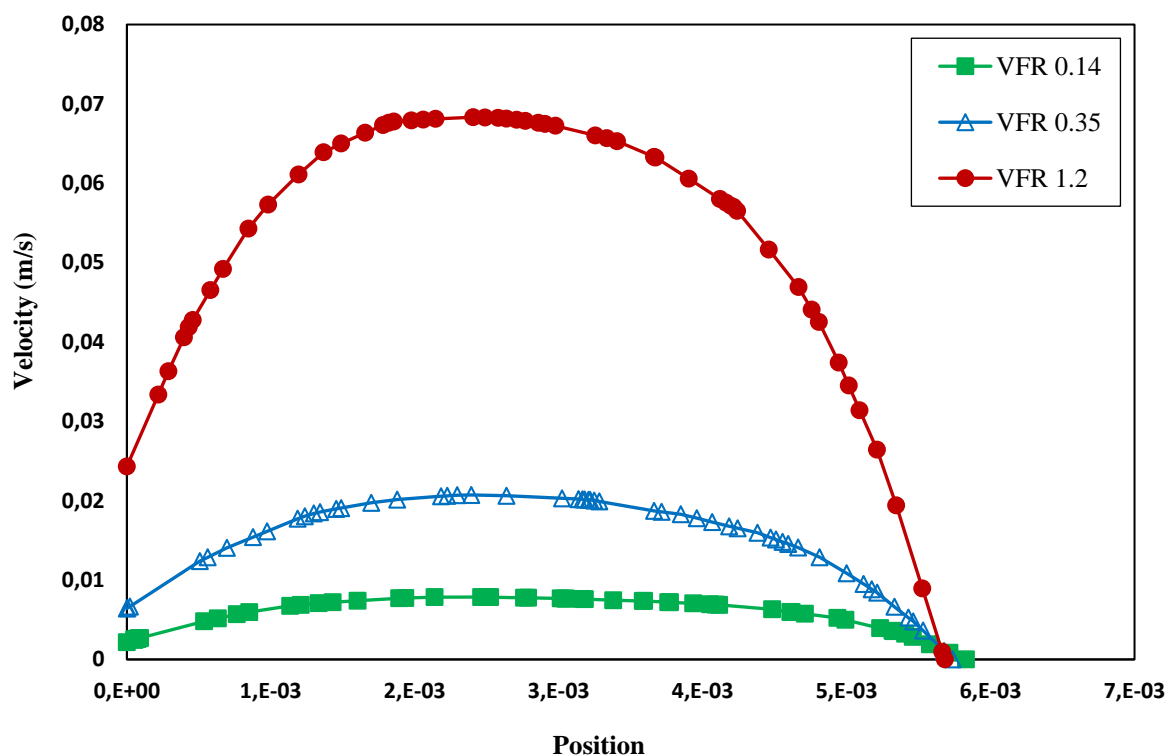


**Fig. 16.** Velocity profile of 0.3 wt% MWCNTs nanofluids at different volume flow rates.

### 4.3. Comparison of the results of TiO<sub>2</sub> and MWCNTs nanofluids

Based on the acquired findings, it can be concluded that at a constant concentration of nanoparticles, the MWCNTs/turbine meter oil nanofluid had a higher pressure drop and friction coefficient than TiO<sub>2</sub>/turbine meter oil nanofluid. This phenomenon occurred due to the larger dimensions of MWCNTs (13 nm) than the TiO<sub>2</sub> nanoparticles (10 nm). The number of particles in the nanofluid containing MWCNTs was greater than the nanofluid containing TiO<sub>2</sub> nanoparticles. Thus, increasing these particles' movement and random motion increased the pressure drop of MWCNTs/turbine meter oil nanofluid. Additionally, due to the shape of the MWCNTs, they were more likely to be agglomerated and be more viscous; accordingly, they increased the pressure drop and coefficient of friction.

Figure 17 shows the velocity profile of nanofluids containing TiO<sub>2</sub> and MWCNTs at different positions. It is observed that nanofluids containing MWCNTs developed faster than

nanofluids containing TiO<sub>2</sub>. Since the viscosity of MWCNTs/turbine meter oil was higher than that of TiO<sub>2</sub>/turbine meter oil, the Reynolds number was further reduced and developed faster.

Toghraei et al. [69] simulated the flow of a fluid containing platinum and copper nanoparticles into a nanochannel. They reported that since the size of platinum particles was larger than copper, the nanofluid containing platinum developed faster.

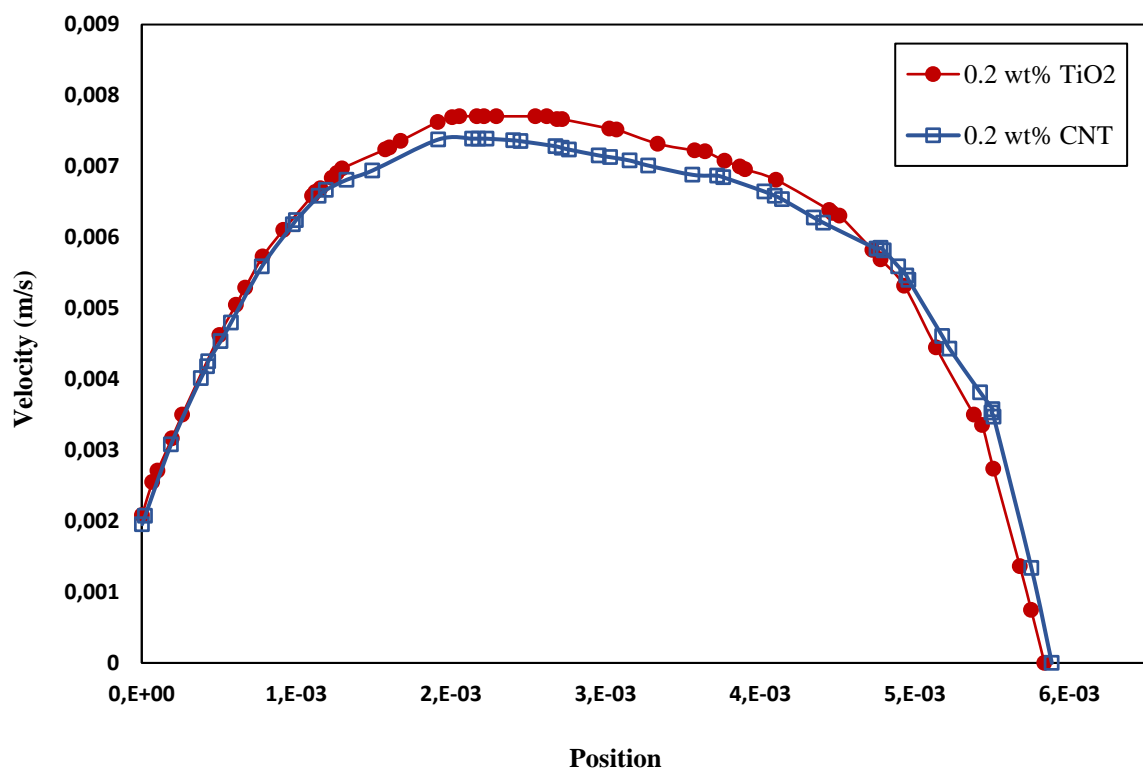


**Fig. 17.** Velocity profile of 0.2 wt% TiO<sub>2</sub> and MWCNTs nanofluids at a flow rate of 0.14

$\frac{cm^3}{s}$  at different positions.

## 5. Conclusion

This simulation aimed to investigate the effect of MWCNTs and TiO<sub>2</sub> nanoparticles on the performance of the gas turbine meter oil. Moreover, the pressure drop and coefficient of friction of TiO<sub>2</sub>/turbine meter oil and MWCNTs/turbine meter oil nanofluids were studied.



With the increase of concentration of nanoparticles, the pressure drop increased due to the higher viscosity of the prepared nanofluids at higher concentrations. Furthermore, As the volume flow rate increased, the nanofluid pressure drop increased. It was further observed that the coefficient of friction increased with the increase of nanoparticles concentration at a constant volume flow rate. Considering each nanofluid, it was concluded that the coefficient of friction was inversely related to the volume flow rate. Concerning the physical characteristics of the pipe, it was reported that at higher concentrations of nanoparticles, a faster fully developed state occurred. Moreover, the MWCNTs/turbine meter oil nanofluids represented a higher coefficient of friction and pressure drops compared to the TiO<sub>2</sub>/turbine meter oil nanofluid.

#### **Author contribution:**

**Atiyeh Aghaei Sarvari:** Investigation, Methodology, Conceptualization, Formal analysis, Writing original draft. **Saeed Zeinali Heris:** Supervision, Conceptualization, Formal analysis, Validation, Review & Editing. **Mousa Mohammadpourfard:**, Review & Editing. **Seyed Borhan Mousavi:**, Formal analysis, Writing original draft. **Patrice Estellé:** Validation, Review & Editing.

## **6. References**

- [1] S. B. Mousavi, S. Z. Heris, and P. Estellé, "Experimental comparison between ZnO and MoS<sub>2</sub> nanoparticles as additives on performance of diesel oil-based nano lubricant," *Scientific reports*, vol. 10, no. 1, pp. 1-17, 2020.
- [2] S. B. Mousavi, S. Z. Heris, and P. Estellé, "Viscosity, tribological and physicochemical features of ZnO and MoS<sub>2</sub> diesel oil-based nanofluids: An experimental study," *Fuel*, vol. 293, p. 120481, 2021.

- [3] Y. Singh, A. Sharma, N. K. Singh, and M. Noor, "Effect of SiC nanoparticles concentration on novel feedstock *Moringa Oleifera* chemically treated with neopentylglycol and their tribological behavior," *Fuel*, vol. 280, p. 118630, 2020.
- [4] A. Boroomandpour, D. Toghraie, and M. Hashemian, "A comprehensive experimental investigation of thermal conductivity of a ternary hybrid nanofluid containing MWCNTs-titania-zinc oxide/water-ethylene glycol (80: 20) as well as binary and mono nanofluids," *Synthetic Metals*, vol. 268, p. 116501, 2020.
- [5] D. Toghraie, N. Sina, N. A. Jolfaei, M. Hajian, and M. Afrand, "Designing an Artificial Neural Network (ANN) to predict the viscosity of Silver/Ethylene glycol nanofluid at different temperatures and volume fraction of nanoparticles," *Physica A: Statistical Mechanics and its Applications*, vol. 534, p. 122142, 2019.
- [6] P. Barnoon, D. Toghraie, F. Eslami, and B. Mehmandoust, "Entropy generation analysis of different nanofluid flows in the space between two concentric horizontal pipes in the presence of magnetic field: single-phase and two-phase approaches," *Computers & Mathematics with Applications*, vol. 77, no. 3, pp. 662-692, 2019.
- [7] F. T. Hong, A. Schneider, and S. M. Sarathy, "Enhanced lubrication by core-shell TiO<sub>2</sub> nanoparticles modified with gallic acid ester," *Tribology International*, vol. 146, p. 106263, 2020.
- [8] A. Samadzadeh and S. Z. Heris, "Effect of stabilization method on the natural convection in an inclined cavity filled with MWCNTs/water nanofluids," *International Communications in Heat and Mass Transfer*, vol. 129, p. 105645, 2021.
- [9] A. Samadzadeh, S. Z. Heris, I. Hashim, and O. Mahian, "An experimental investigation on natural convection of non-covalently functionalized MWCNTs nanofluids: effects of aspect ratio and inclination angle," *International Communications in Heat and Mass Transfer*, vol. 111, p. 104473, 2020.

- [10] S. Z. Heris, M. Fallahi, M. Shanbedi, and A. Amiri, "Heat transfer performance of two-phase closed thermosyphon with oxidized CNT/water nanofluids," *Heat and Mass Transfer*, vol. 52, no. 1, pp. 85-93, 2016.
- [11] M. H. Aghahadi, M. Niknejadi, and D. Toghraie, "An experimental study on the rheological behavior of hybrid Tungsten oxide (WO<sub>3</sub>)-MWCNTs/engine oil Newtonian nanofluids," *Journal of Molecular Structure*, vol. 1197, pp. 497-507, 2019.
- [12] F. Soltani, D. Toghraie, and A. Karimipour, "Experimental measurements of thermal conductivity of engine oil-based hybrid and mono nanofluids with tungsten oxide (WO<sub>3</sub>) and MWCNTs inclusions," *Powder Technology*, vol. 371, pp. 37-44, 2020.
- [13] P. Sreedevi and P. S. Reddy, "Entropy generation and heat transfer analysis of alumina and carbon nanotubes based hybrid nanofluid inside a cavity," *Physica Scripta*, vol. 96, no. 8, p. 085210, 2021.
- [14] M. Doğan, A. Selek, O. Turhan, B. K. Kızılduman, and Z. Bicil, "Different functional groups functionalized hexagonal boron nitride (h-BN) nanoparticles and multi-walled carbon nanotubes (MWCNT) for hydrogen storage," *Fuel*, vol. 303, p. 121335, 2021.
- [15] E. M. C. Contreras and E. P. Bandarra Filho, "HEAT TRANSFER PERFORMANCE OF AN AUTOMOTIVE RADIATOR WITH MWCNT NANOFLUID COOLING IN A HIGH OPERATING TEMPERATURE RANGE," *Applied Thermal Engineering*, p. 118149, 2022.
- [16] Z. Said, P. Sharma, L. S. Sundar, A. Afzal, and C. Li, "Synthesis, stability, thermophysical properties and AI approach for predictive modelling of Fe<sub>3</sub>O<sub>4</sub> coated MWCNT hybrid nanofluids," *Journal of Molecular Liquids*, vol. 340, p. 117291, 2021.
- [17] W. He *et al.*, "Using of artificial neural networks (ANNs) to predict the thermal conductivity of zinc oxide–silver (50%–50%)/water hybrid Newtonian nanofluid," *International Communications in Heat and Mass Transfer*, vol. 116, p. 104645, 2020.

- [18] S.-R. Yan, D. Toghraie, L. A. Abdulkareem, A. a. Alizadeh, P. Barnoon, and M. Afrand, "The rheological behavior of MWCNTs–ZnO/Water–Ethylene glycol hybrid non-Newtonian nanofluid by using of an experimental investigation," *Journal of Materials Research and Technology*, vol. 9, no. 4, pp. 8401-8406, 2020.
- [19] S. Rostami, D. Toghraie, B. Shabani, N. Sina, and P. Barnoon, "Measurement of the thermal conductivity of MWCNT-CuO/water hybrid nanofluid using artificial neural networks (ANNs)," *Journal of Thermal Analysis and Calorimetry*, vol. 143, no. 2, pp. 1097-1105, 2021.
- [20] P. S. Reddy and P. Sreedevi, "Flow and heat transfer analysis of carbon nanotubes based nanofluid flow inside a cavity with modified Fourier heat flux," *Physica Scripta*, vol. 96, no. 5, p. 055215, 2021.
- [21] P. S. Reddy, P. Sreedevi, and K. V. S. Rao, "Impact of heat generation/absorption on heat and mass transfer of nanofluid over rotating disk filled with carbon nanotubes," *International Journal of Numerical Methods for Heat & Fluid Flow*, 2020.
- [22] P. Sreedevi and P. Sudarsana Reddy, "Impact of Convective Boundary Condition on Heat and Mass Transfer of Nanofluid Flow Over a Thin Needle Filled with Carbon Nanotubes," *Journal of Nanofluids*, vol. 9, no. 4, pp. 282-292, 2020.
- [23] P. Sudarsana Reddy, K. Jyothi, and M. Suryanarayana Reddy, "Flow and heat transfer analysis of carbon nanotubes-based Maxwell nanofluid flow driven by rotating stretchable disks with thermal radiation," *Journal of the Brazilian Society of Mechanical Sciences and Engineering*, vol. 40, no. 12, pp. 1-16, 2018.
- [24] Z. S. Mahmoudabadi, A. Rashidi, and A. Tavasoli, "Synthesis of two-dimensional TiO<sub>2</sub>@ multi-walled carbon nanotube nanocomposites as smart nanocatalyst for ultra-deep oxidative desulfurization of liquid fuel: Optimization via response surface methodology," *Fuel*, vol. 306, p. 121635, 2021.

- [25] Y. Singh, D. Singh, A. Singla, A. Sharma, and N. K. Singh, "Chemical modification of juliflora oil with trimethylolpropane (TMP) and effect of TiO<sub>2</sub> nanoparticles concentration during tribological investigation," *Fuel*, vol. 280, p. 118704, 2020.
- [26] M. Valihesari, V. Pirouzfar, F. Ommi, and F. Zamankhan, "Investigating the effect of Fe<sub>2</sub>O<sub>3</sub> and TiO<sub>2</sub> nanoparticle and engine variables on the gasoline engine performance through statistical analysis," *Fuel*, vol. 254, p. 115618, 2019.
- [27] J. Hou, H. Yang, B. He, J. Ma, Y. Lu, and Q. Wang, "High photocatalytic performance of hydrogen evolution and dye degradation enabled by CeO<sub>2</sub> modified TiO<sub>2</sub> nanotube arrays," *Fuel*, vol. 310, p. 122364, 2022.
- [28] B. Ruhani, P. Barnoon, and D. Toghraie, "Statistical investigation for developing a new model for rheological behavior of Silica–ethylene glycol/Water hybrid Newtonian nanofluid using experimental data," *Physica A: Statistical Mechanics and Its Applications*, vol. 525, pp. 616-627, 2019.
- [29] P. Sreedevi and P. S. Reddy, "Effect of magnetic field and thermal radiation on natural convection in a square cavity filled with TiO<sub>2</sub> nanoparticles using Tiwari-Das nanofluid model," *Alexandria Engineering Journal*, vol. 61, no. 2, pp. 1529-1541, 2022.
- [30] S. Rostami, S. Mahdavi, M. Alinezhadfar, and A. Mohseni, "Tribological and corrosion behavior of electrochemically deposited Co/TiO<sub>2</sub> micro/nano-composite coatings," *Surface and Coatings Technology*, vol. 423, p. 127591, 2021.
- [31] W. H. Kan and L. Chang, "The mechanisms behind the tribological behaviour of polymer matrix composites reinforced with TiO<sub>2</sub> nanoparticles," *Wear*, vol. 474, p. 203754, 2021.
- [32] M. S. Park, C. S. Lee, J. H. Lee, D. Y. Ryu, and J. H. Kim, "Dissolution–precipitation approach for long-term stable low-friction composites consisting of mesoporous TiO<sub>2</sub>

nanospheres and carbon black in Poly (Vinylidene fluoride) matrix," *Tribology International*, vol. 145, p. 106187, 2020.

[33] A. Shahsavar, S. Khanmohammadi, D. Toghraie, and H. Salihepour, "Experimental investigation and develop ANNs by introducing the suitable architectures and training algorithms supported by sensitivity analysis: measure thermal conductivity and viscosity for liquid paraffin based nanofluid containing Al<sub>2</sub>O<sub>3</sub> nanoparticles," *Journal of Molecular Liquids*, vol. 276, pp. 850-860, 2019.

[34] I. Ali *et al.*, "Advances in carbon nanomaterials as lubricants modifiers," *Journal of molecular liquids*, vol. 279, pp. 251-266, 2019.

[35] Y. Singh, N. K. Singh, A. Sharma, A. Singla, D. Singh, and E. Abd Rahim, "Effect of ZnO nanoparticles concentration as additives to the epoxidized Euphorbia Lathyris oil and their tribological characterization," *Fuel*, vol. 285, p. 119148, 2021.

[36] M. Heidari, M. Tahmasebpour, A. Antzaras, and A. A. Lemonidou, "CO<sub>2</sub> capture and fluidity performance of CaO-based sorbents: Effect of Zr, Al and Ce additives in tri-, bi-and mono-metallic configurations," *Process Safety and Environmental Protection*, vol. 144, pp. 349-365, 2020.

[37] M. Heidari, M. Tahmasebpour, S. B. Mousavi, and C. Pevida, "CO<sub>2</sub> capture activity of a novel CaO adsorbent stabilized with (ZrO<sub>2</sub>+ Al<sub>2</sub>O<sub>3</sub>+ CeO<sub>2</sub>)-based additive under mild and realistic calcium looping conditions," *Journal of CO<sub>2</sub> Utilization*, vol. 53, p. 101747, 2021.

[38] S. S. Seyedi, M. R. Shabgard, S. B. Mousavi, and S. Z. Heris, "The impact of SiC, Al<sub>2</sub>O<sub>3</sub>, and B<sub>2</sub>O<sub>3</sub> abrasive particles and temperature on wear characteristics of 18Ni (300) maraging steel in abrasive flow machining (AFM)," *International Journal of Hydrogen Energy*, 2021.

- [39] Y. Singh and E. Abd Rahim, "Michelia Champaca: Sustainable novel non-edible oil as nano based bio-lubricant with tribological investigation," *fuel*, vol. 282, p. 118830, 2020.
- [40] S. K. Chaurasia, N. K. Singh, and L. K. Singh, "Friction and wear behavior of chemically modified Sal (Shorea Robusta) oil for bio based lubricant application with effect of CuO nanoparticles," *fuel*, vol. 282, p. 118762, 2020.
- [41] B. A. Vardhaman, M. Amarnath, J. Ramkumar, and K. Mondal, "Enhanced tribological performances of zinc oxide/MWCNTs hybrid nanomaterials as the effective lubricant additive in engine oil," *Materials Chemistry and Physics*, vol. 253, p. 123447, 2020.
- [42] B. Wang, Q. Fu, L. Sun, Y. Lu, and Y. Liu, "Improving the tribological performance of carbon fiber reinforced resin composite by grafting MWCNT and GNPs on fiber surface," *Materials Letters*, vol. 306, p. 130953, 2022.
- [43] C. Almeida *et al.*, "Experimental Studies on Thermophysical and Electrical Properties of Graphene–Transformer Oil Nanofluid," *Fluids*, vol. 5, no. 4, p. 172, 2020.
- [44] H. Akbarpour, A. Rashidi, M. Mirjalili, and A. Nazari, "Comparison of the conductive properties of polyester/viscose fabric treated with Cu nanoparticle and MWCNT s," *Journal of Nanostructure in Chemistry*, vol. 9, no. 4, pp. 335-348, 2019.
- [45] A. S. Al-Janabi, M. Hussin, and M. Abdullah, "Stability, thermal conductivity and rheological properties of graphene and MWCNT in nanolubricant using additive surfactants," *Case Studies in Thermal Engineering*, vol. 28, p. 101607, 2021.
- [46] H. Rangaswamy, M. P. G. Chandrashekarappa, D. Y. Pimenov, K. Giasin, and S. Wojciechowski, "Experimental investigation and optimization of compression moulding parameters for MWCNT/glass/kevlar/epoxy composites on mechanical and tribological properties," *journal of materials research and technology*, vol. 15, pp. 327-341, 2021.

- 626 [47] M. Padhan, U. Marathe, and J. Bijwe, "Tribology of Poly (etherketone) composites  
627 based on nano-particles of solid lubricants," *Composites Part B: Engineering*, p.  
628 108323, 2020.
- 629 [48] R. de la Cruz Parejas, F. J. Moura, R. R. de Avillez, and P. R. de Souza Mendes, "Effects  
630 of Al<sub>2</sub>O<sub>3</sub>-NiO, TiO<sub>2</sub> and (Mg, Ni) O particles on the viscosity of heavy oil during  
631 aquathermolysis," *Colloids and Surfaces A: Physicochemical and Engineering Aspects*,  
632 vol. 625, p. 126863, 2021.
- 633 [49] A. M. Abdullah *et al.*, "Tailoring the viscosity of water and ethylene glycol based TiO<sub>2</sub>  
634 nanofluids," *Journal of Molecular Liquids*, vol. 297, p. 111982, 2020.
- 635 [50] V. V. Wanatasanapan, M. Abdullah, and P. Gunnasegaran, "Effect of TiO<sub>2</sub>-Al<sub>2</sub>O<sub>3</sub>  
636 nanoparticle mixing ratio on the thermal conductivity, rheological properties, and  
637 dynamic viscosity of water-based hybrid nanofluid," *Journal of Materials Research  
638 and Technology*, vol. 9, no. 6, pp. 13781-13792, 2020.
- 639 [51] S. Z. Heris, F. Farzin, and H. Sardarabadi, "Experimental comparison among thermal  
640 characteristics of three metal oxide nanoparticles/turbine oil-based nanofluids under  
641 laminar flow regime," *International Journal of Thermophysics*, vol. 36, no. 4, pp. 760-  
642 782, 2015.
- 643 [52] M. Hosseinzadeh, S. Z. Heris, A. Beheshti, and M. Shanbedi, "Convective heat transfer  
644 and friction factor of aqueous Fe<sub>3</sub>O<sub>4</sub> nanofluid flow under laminar regime," *Journal  
645 of Thermal Analysis and Calorimetry*, vol. 124, no. 2, pp. 827-838, 2016.
- 646 [53] M. K. A. Ali, H. Xianjun, R. F. Turkson, Z. Peng, and X. Chen, "Enhancing the  
647 thermophysical properties and tribological behaviour of engine oils using nano-  
648 lubricant additives," *RSC advances*, vol. 6, no. 81, pp. 77913-77924, 2016.



- [54] F. L. G. Borda, S. J. R. de Oliveira, L. M. S. M. Lazaro, and A. J. K. Leiróz, "Experimental investigation of the tribological behavior of lubricants with additive containing copper nanoparticles," *Tribology International*, vol. 117, pp. 52-58, 2018.
- [55] M. Laad and V. K. S. Jatti, "Titanium oxide nanoparticles as additives in engine oil," *Journal of King Saud University-Engineering Sciences*, vol. 30, no. 2, pp. 116-122, 2018.
- [56] F. Curà, A. Mura, and F. Adamo, "Experimental investigation about tribological performance of grapheme-nanoplatelets as additive for lubricants," *Procedia Structural Integrity*, vol. 12, pp. 44-51, 2018.
- [57] A. A. Hussien, N. M. Yusop, M. Z. Abdullah, A.-N. Moh'd A, and M. Khavarian, "Study on convective heat transfer and pressure drop of MWCNTs/water nanofluid in mini-tube," *Journal of Thermal Analysis and Calorimetry*, vol. 135, no. 1, pp. 123-132, 2019.
- [58] A. Naddaf, S. Z. Heris, and B. Pouladi, "An experimental study on heat transfer performance and pressure drop of nanofluids using graphene and multi-walled carbon nanotubes based on diesel oil," *Powder Technology*, vol. 352, pp. 369-380, 2019.
- [59] S. B. Mousavi, S. Z. Heris, and M. G. Hosseini, "Experimental investigation of MoS<sub>2</sub>/diesel oil nanofluid thermophysical and rheological properties," *International Communications in Heat and Mass Transfer*, vol. 108, p. 104298, 2019.
- [60] R. K. Ajeel and W.-I. Salim, "Experimental assessment of heat transfer and pressure drop of nanofluid as a coolant in corrugated channels," *Journal of Thermal Analysis and Calorimetry*, pp. 1-13, 2020.
- [61] H. Pourpasha, S. Z. Heris, O. Mahian, and S. Wongwises, "The effect of multi-wall carbon nanotubes/turbine meter oil nanofluid concentration on the thermophysical properties of lubricants," *Powder Technology*, vol. 367, pp. 133-142, 2020.

- [62] E. S. Menon, *Working Guide to Pump and Pumping Stations: Calculations and Simulations*. Gulf Professional Publishing, 2009.
- [63] M. Kutz, *Mechanical Engineers' Handbook, Volume 4: Energy and Power*. John Wiley & Sons, 2015.
- [64] M. Everts and J. P. Meyer, "Laminar hydrodynamic and thermal entrance lengths for simultaneously hydrodynamically and thermally developing forced and mixed convective flows in horizontal tubes," *Experimental Thermal and Fluid Science*, vol. 118, p. 110153, 2020.
- [65] P. Samira, Z. H. Saeed, S. Motahare, and K. Mostafa, "Pressure drop and thermal performance of CuO/ethylene glycol (60%)-water (40%) nanofluid in car radiator," *Korean journal of chemical engineering*, vol. 32, no. 4, pp. 609-616, 2015.
- [66] S. B. Mousavi and S. Z. Heris, "Experimental investigation of ZnO nanoparticles effects on thermophysical and tribological properties of diesel oil," *International Journal of Hydrogen Energy*, vol. 45, no. 43, pp. 23603-23614, 2020.
- [67] M. Gholinia, S. Gholinia, K. Hosseinzadeh, and D. Ganji, "Investigation on ethylene glycol nano fluid flow over a vertical permeable circular cylinder under effect of magnetic field," *Results in Physics*, vol. 9, pp. 1525-1533, 2018.
- [68] L. Bao, C. Zhong, P. Jie, and Y. Hou, "The effect of nanoparticle size and nanoparticle aggregation on the flow characteristics of nanofluids by molecular dynamics simulation," *Advances in Mechanical Engineering*, vol. 11, no. 11, p. 1687814019889486, 2019.
- [69] D. Toghraie, M. Mokhtari, and M. Afrand, "Molecular dynamic simulation of copper and platinum nanoparticles Poiseuille flow in a nanochannels," *Physica E: Low-dimensional Systems and Nanostructures*, vol. 84, pp. 152-161, 2016.